HHS Public Access

Author manuscript

Nano Lett. Author manuscript; available in PMC 2020 November 14.

Published in final edited form as:

Nano Lett. 2020 October 14; 20(10): 7783–7792. doi:10.1021/acs.nanolett.0c03414.

Cancer Immunotherapy via Targeting Cancer Stem Cells Using Vaccine Nanodiscs

Alireza Hassani Najafabadi[¶],
Department of Pharmaceutical Sciences and Biointerfaces Institute, University of Michigan, Ann Arbor, Michigan 48109, United States

Jing Zhang[¶],
Department of Surgery, University of Michigan, Ann Arbor, Michigan 48109, United States; Department of Medical Oncology, Hubei Cancer Hospital, Tongji Medical College, Huazhong University of Science and Technology, Wuhan, Hubei 430079, China

Marisa E. Aikins,
Department of Pharmaceutical Sciences and Biointerfaces Institute, University of Michigan, Ann Arbor, Michigan 48109, United States

Zeynab Izadi Najaf Abadi,
Department of Pharmaceutical Sciences and Biointerfaces Institute, University of Michigan, Ann Arbor, Michigan 48109, United States

Fei Liao,
Department of Surgery, University of Michigan, Ann Arbor, Michigan 48109, United States; Gastroenterology Department, Renmin Hospital of Wuhan University, Wuhan, Hubei 430060, China

You Qin,
Department of Surgery, University of Michigan, Ann Arbor, Michigan 48109, United States; Cancer Center, Union Hospital, Tongji Medical College, Huazhong University of Science and Technology, Wuhan, Hubei 430022, China

Emeka B. Okeke,

Corresponding Authors: moonjj@med.umich.edu; qiaoli@med.umich.edu.
[¶]A.H.N. and J.Z. contributed equally.

Author Contributions

A.H.N., J.Z., M.S.W., Q.L., and J.J.M. designed the experiments. A.H.N., J.Z., Z.I.N.A., Y.Q., and F.L. performed the experiments. L.M.S. and Y.X. contributed to the ELISPOT assays. M.E.A., E.B.O., J.N., and A.S. contributed to the preparation and characterization of vaccine nanodiscs. D.A. contributed to the flow cytometry analyses. P.L. and T.H. contributed to the animal studies. A.H.N., J.Z., Z.I.N.A., A.E.C., Q.L., and J.J.M. analyzed the data. A.H.N., M.E.A., and J.J.M. wrote the paper.

Supporting Information

The Supporting Information is available free of charge at https://pubs.acs.org/doi/10.1021/acs.nanolett.0c03414.
ND delivery to dLNs (Figure S1), effects of ALDH vaccination on HSCs and animal body weight (Figure S2), serum biochemical markers after ND vaccination (Table S1), and complete blood counts after ND vaccination (Table S2) (PDF)

Complete contact information is available at: https://pubs.acs.org/10.1021/acs.nanolett.0c03414

The authors declare the following competing financial interest(s): A patent application for nanodisc vaccines has been filed with J.J.M., A.S., A.H.N., and J.N. as inventors. J.J.M. and A.S. are cofounders of EVOQ Therapeutics, LLC, which develops the nanodisc technology for vaccine applications.

Department of Pharmaceutical Sciences and Biointerfaces Institute, University of Michigan, Ann Arbor, Michigan 48109, United States

Lindsay M. Scheetz,
Department of Pharmaceutical Sciences and Biointerfaces Institute, University of Michigan, Ann Arbor, Michigan 48109, United States

Jutaek Nam,
Department of Pharmaceutical Sciences and Biointerfaces Institute, University of Michigan, Ann Arbor, Michigan 48109, United States

Yao Xu,
Department of Pharmaceutical Sciences and Biointerfaces Institute, University of Michigan, Ann Arbor, Michigan 48109, United States

David Adams,
Biomedical Research Core Facilities, University of Michigan, Ann Arbor, Michigan 48109, United States

Patrick Lester,
Unit for Laboratory Animal Medicine, University of Michigan, Ann Arbor, Michigan 48109, United States

Taryn Hetrick,
Unit for Laboratory Animal Medicine, University of Michigan, Ann Arbor, Michigan 48109, United States

Anna Schwendeman,
Department of Pharmaceutical Sciences and Biointerfaces Institute, University of Michigan, Ann Arbor, Michigan 48109, United States

Max S. Wicha,
Department of Surgery, University of Michigan, Ann Arbor, Michigan 48109, United States

Alfred E. Chang,
Department of Surgery, University of Michigan, Ann Arbor, Michigan 48109, United States

Qiao Li,
Department of Surgery, University of Michigan, Ann Arbor, Michigan 48109, United States

James J. Moon
Department of Pharmaceutical Sciences, Biointerfaces Institute, and Department of Biomedical Engineering, University of Michigan, Ann Arbor, Michigan 48109, United States

Abstract

Cancer stem cells (CSCs) proliferate extensively and drive tumor metastasis and recurrence. CSCs have been identified in over 20 cancer types to date, but it remains unknown how to target and eliminate CSCs in vivo. Aldehyde dehydrogenase (ALDH) is a marker that has been used extensively for isolating CSCs. Here we present a novel approach to target and reduce the frequency of $ALDH^{high}$ CSCs by vaccination against ALDH. We have identified ALDH1-A1 and ALDH1-A3 epitopes from CSCs and developed synthetic high-density lipoprotein nanodiscs for

vaccination against ALDH^{high} CSCs. Nanodiscs increased antigen trafficking to lymph nodes and generated robust ALDH-specific T cell responses. Nanodisc vaccination against ALDH^{high} CSCs combined with anti-PD-L1 therapy exerted potent antitumor efficacy and prolonged animal survival in multiple murine models. Overall, this is the first demonstration of a simple nanovaccine strategy against CSCs and may lead to new avenues for cancer immunotherapy against CSCs.

Graphical Abstract

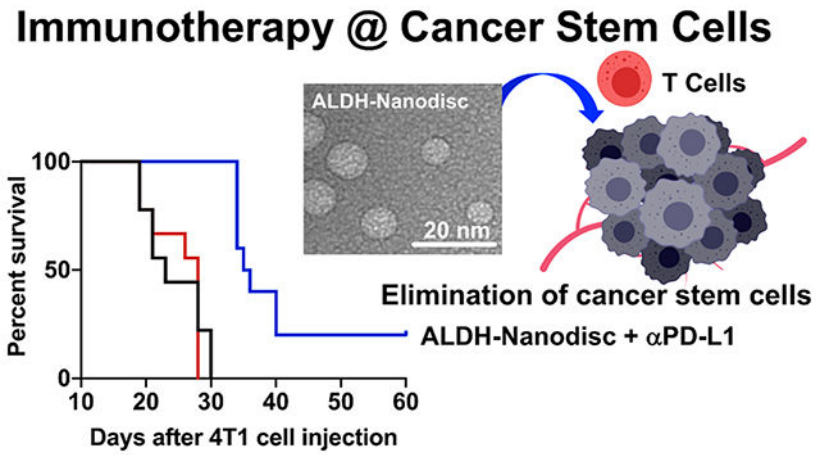

Keywords

Cancer stem cells; cancer vaccine; breast cancer; melanoma; aldehyde dehydrogenase

Cancer is one of the most significant causes of death worldwide despite decades of research. Standard treatments for patients with solid malignancies include surgical resection, chemotherapy, and radiation therapy; however, their efficacy is limited by tumor recurrence and metastasis. One mechanism for tumor recurrence is cancer stem cells (CSCs), which are a small fraction of cancer cells that self-renew, mediate tumor growth, and contribute to tumor metastasis.[1–5] Unlike differentiated cancer cells, CSCs exist in a mostly inactive cell cycle, making them resistant to standard cytotoxic drugs designed to target rapidly dividing cells. Thus, CSCs are considered one of the key factors that drive chemoresistance, tumor relapse, and metastasis.[3–5]

Aldehyde dehydrogenase (ALDH), which is known to detoxify intracellular aldehydes through an oxidation process, has been extensively used as a functional biomarker to isolate CSCs from more than 20 cancer types.[6–11] We have previously shown that dendritic cells (DCs) pulsed with cell lysate from ALDH^{high} CSCs generated CSC-specific T cells and humoral immune responses and that anti-PD-L1 immunoglobulin G (IgG) augmented these adaptive immune responses.[12–14] Despite these promising results, this approach has been limited by the requirement for isolation of a sufficient number of patient-specific CSCs and suboptimal clinical efficacy of DC vaccines.[15] On the other hand, cancer immunotherapy based on immune checkpoint blockade (ICB) is now established as a major pillar in cancer therapies.[16–18] However, current ICB therapy benefits only a small group of cancer patients, with response rates of 10–30% reported in the clinic.[18–20] Importantly, recent studies have

indicated that CSCs may contribute to immune resistance by employing multiple mechanisms to evade immune surveillance, including expression of immunosuppressive genes and cytokines.[21–23] However, it remains unknown how to selectively target and eliminate CSCs.

To overcome these critical challenges, we sought to identify new CSC antigens and utilize them to elicit T cell immunity against CSCs (Figure 1A). ALDH constitutes a family of over 20 members, and we and others have previously shown that ALDH1-A1 and ALDH1-A3 are the primary isoforms found in human CSCs of melanoma and breast cancer patients.[24–27] Hence, we have focused on antigenic sequences predicted to be immunogenic from human ALDH1-A1 and ALDH1-A3 and identified ALDH1-A1$_{88–96}$ and ALDH1-A3$_{99–107}$ as promising ALDH epitopes with sequence homology in mice. Using these epitopes (termed ALDH-A1 and ALDH-A3 peptides), we have developed a nanoparticle vaccine system to deliver ALDH epitope peptides to antigen-presenting cells (APCs) and elicit T cell responses against ALDH^{high} CSCs. Our approach is based on synthetic high-density lipoprotein nanodiscs (NDs) composed of apolipoprotein-A1-mimetic peptide (22A) and phospholipids.[28,29] These NDs have attractive features for vaccination against CSCs: (1) NDs with a small diameter (~10 nm) allow direct access to draining lymph nodes (dLNs) after subcutaneous (sc) administration; (2) NDs mediate codelivery of antigen and adjuvant to DCs in dLNs; (3) NDs promote antigen processing and presentation on DCs; and (4) NDs are safe, well-characterized, and amenable for scalable manufacturing.[28,29] Here we report that NDs coloaded with ALDH antigen peptides and immunostimulatory molecules induce robust ALDH-specific T cell responses, reduce ALDH^{high} CSCs, and exert potent antitumor efficacy in murine models of D5 melanoma and 4T1 breast cancer (Figure 1A).

Specifically, as ALDH1-A1 and ALDH1-A3 are the primary isoforms found in human CSCs of melanoma and breast cancer patients,[24–27] we analyzed ALDH-A1 and ALDH-A3 sequences for predicted binding to major histocompatibility complex-I (MHC-I) using an MHC-binding prediction tool (IEBD) and identified ALDH1-A1$_{88–96}$ and ALDH1-A3$_{99–107}$ with low predicted IC_{50} values as promising ALDH epitopes with sequence homology in mice. Using these ALDH-A1 and ALDH-A3 epitope peptides, we synthesized NDs coloaded with ALDH antigens and CpG (a TLR-9 agonist). Briefly, NDs were synthesized by mixing 1,2-dimyristoyl-*sn*-glycerol-3-phosphocholine (DMPC) and 22A followed by lyophilization, rehydration, and heating/cooling cycles. Afterward, ALDH antigen peptides (ALDH-A1 and ALDH-A3) premodified with a cysteine at the N-terminus were conjugated with 1,2-dioleoyl-*sn*-glycero-3-phosphoethanolamine-*N*-[3-(2-pyridyldithio)propionate] (DOPE-PDP) and then added to preformed NDs to produce antigen-loaded NDs. Quantification with HPLC/MS showed highly efficient conjugation of ALDH antigen peptides to DOPE lipid and subsequent incorporation of the lipid–peptide conjugates into NDs (>90% efficiency for both) (Figure 1B–D). HPLC chromatograms showed a reduction in the area under the curve (AUC) for the DOPE-PDP peak after mixing with cysteine-modified ALDH-A1 or ALDH-A3 peptides, indicating successful conjugation, and this reduction in AUC was accompanied by the appearance of the lipid–peptide conjugate peak at 21.9 min (Figure 1D). Subsequently, cholesterol-modified CpG1826 (cho-CpG) was incubated with antigen-loaded NDs by simple mixing at a DMPC:cho-CpG weight ratio of 50:1. Gel-permeation chromatography (GPC) analysis showed >90% cho-CpG loading into

NDs, resulting in the formation of NDs coloaded with CpG and either ALDH-A1 or ALDH-A3 peptide, termed (ALDH-A1-CpG)-ND and (ALDH-A3-CpG)-ND, respectively (Figure 1E,F). Dynamic light scattering (DLS) revealed that the addition of antigen and cho-CpG to blank NDs did not significantly increase the size of the resulting NDs (Figure 1G). (ALDH-A1-CpG)-ND and (ALDH-A3-CpG)-ND had comparable particle sizes ranging from 9 to 13 nm, a polydispersity index of 0.20 ± 0.02, and slightly positive charges of 2.8 ± 0.1 and 3.4 ± 0.3 mV, respectively. The transmission electron microscopy (TEM) images showed that the NDs had an average diameter of 10 ± 3 nm (Figure 1H), in line with the DLS results.

To study the lymphatic delivery of antigen in vivo, C57BL/6 mice were immunized sc at the tail base with ALDH-A1 peptide fluorescently tagged with tetramethylrhodamine (TMR) in soluble form or ND form (Figure 2A). Administration of soluble ALDH-A1-TMR peptide resulted in minimal TMR signal in inguinal dLNs after 24 h (Figure 2B,C). This is consistent with literature reports of limited lymphatic delivery of short soluble peptides after sc administration due to systemic dissemination of low-molecular-weight peptides and direct antigen binding to non-APCs at the injection site.[30] In contrast, administration of (ALDH-A1-TMR)-ND led to a significantly higher TMR signal in inguinal dLNs compared with the soluble ALDH-A1-TMR group ($p < 0.0001$; Figure 2B,C). Next, we examined antigen uptake by APCs in dLNs by flow cytometry analysis. Consistent with the above results, (ALDH-A1-TMR)-ND promoted cellular uptake of antigen, significantly increasing the mean fluorescence intensity (MFI) of TMR among $CD11c^+$ DCs (5.9-fold, $p < 0.01$), $B220^+$ B cells (7.9-fold, $p < 0.001$), and $F4/80^+$ macrophages (6.3-fold, $p < 0.001$) as well as the percentages of TMR+ APCs compared with the soluble ALDH-A1-TMR group (Figures 2D–F and S1). Taken together, these results showed that NDs efficiently delivered ALDH peptide to dLNs and promoted antigen uptake by APCs in dLNs, which are prerequisites for the induction of T cell responses against these ALDH peptides.

Having shown that NDs increase antigen delivery to LNs, we next investigated their efficacy as a therapeutic vaccine in a syngeneic murine model of D5 melanoma, which is known to harbor $ALDH^{high}$ CSCs.[12] C57BL/6 mice were inoculated sc in the flank with 5×10^4 D5 melanoma cells. On day 1, mice were immunized sc at the tail base with ALDH-A1, ALDH-A3, and CpG as either a soluble mixture or an (ALDH-A1/A3-CpG)-ND formulation (Figure 3A). (ALDH-A1/A3-CpG)-ND denotes a pooled mixture of NDs carrying CpG and either ALDH-A1 or ALDH-A3 peptide, each loaded in separate NDs. On day 8, a boost vaccination was administered, and mice were monitored for D5 tumor growth. Vaccination with soluble peptide mixture + CpG had no impact on D5 tumor growth or animal survival compared with the PBS control group (Figure 3B–D). In contrast, ND vaccination significantly slowed tumor growth ($p < 0.0001$; Figure 3B,C) and significantly prolonged the animal survival ($p < 0.001$; Figure 3D) compared with soluble peptide vaccination. To further amplify the antitumor immunity by blocking the immunosuppressive PD-1/PD-L1 pathway, a subset of animals also received intraperitoneal (ip) administration of anti-PD-L1 IgG. The addition of anti-PD-L1 IgG therapy augmented the antitumor efficacy of the NDs, leading to enhanced tumor growth suppression and extension of the animal survival ($p < 0.001$; Figure 3B–D). Moreover, anti-PD-L1 IgG therapy also improved soluble peptide vaccination, enhancing tumor growth inhibition and animal survival to a similar level as the ND-vaccine-alone group (Figure 3B–D). We analyzed a subset of tumor tissues on day 23 to

quantify the frequency of ALDH^{high} D5 CSCs. ND vaccination combined with anti-PD-L1 IgG therapy significantly reduced the frequency of ALDH^{high} D5 CSCs compared with the PBS control ($p < 0.05$; Figure 3E).

Next, we examined the impact of ND vaccination on ALDH-specific T cell responses. D5 tumor-bearing mice were treated as shown in Figure 3A, and immunological assays were performed on day 15. Soluble vaccine with or without anti-PD-L1 IgG failed to generate a detectable level of ALDH-specific CD8$^+$ T cell responses in peripheral blood. In contrast, mice treated with (ALDH-A1/A3-CpG)-ND plus anti-PD-L1 IgG elicited robust ALDH-specific CD8$^+$ T cell responses with 62-fold ($p < 0.0001$) and 44-fold ($p < 0.05$) higher frequency of ALDH-A1-tetramer+ and ALDH-A3-tetramer+ CD8$^+$ T cells compared with soluble vaccine plus anti-PD-L1 IgG (Figure 4A–C). ND vaccination combined with anti-PD-L1 therapy also induced robust IFN-γ^+ CD8$^+$ and CD4$^+$ T cell responses, as evidenced by intracellular cytokine staining of peripheral blood mononuclear cells (PBMCs) restimulated with ALDH-A1/A3 peptides (Figure 4D,E). To further delineate the magnitude of T cell responses against ALDH-A1 and ALDH-A3, we performed an interferon γ (IFN-γ) ELISPOT assay using PBMCs restimulated with individual epitopes. Compared with soluble vaccine plus anti-PD-L1 IgG, ND vaccination plus anti-PD-L1 IgG generated 3.9-fold, 4.2-fold, and 7.5-fold higher IFN-γ^+ T cell responses against ALDH-A1, ALDH-A3, and the mixture of two peptides, respectively ($p < 0.0001$; Figure 4F). Moreover, mice immunized with (ALDH-A1/A3-CpG)-ND or soluble ALDH-A1/A3+CpG did not exhibit any signs of toxicity, as they all had normal numbers of hematopoietic stem cells (HSCs) (Lin$^-$c-Kit$^+$Sca-1$^+$) and long-term HSCs (LT-HSCs) (Lin$^-$c-Kit$^+$Sca-1$^+$CD34$^-$)[31] in bone marrow as well as normal animal body weight, blood chemistry, and complete blood cell counts (Figure S2 and Tables S1 and S2). Taken together, these results show that ND vaccination generates robust ALDH-specific T cell responses in a safe and effective manner and exerts potent antitumor efficacy in combination with anti-PD-L1 IgG therapy.

Next, we sought to confirm our results in a second tumor model. The 4T1 cell line is a highly invasive model of mammary carcinoma that is resistant to conventional ICB therapies[32] and is widely used to study CSCs.[33,34] BALB/c mice were inoculated with 10^4 syngeneic 4T1 cells in the mammary fat pad, and the animals were immunized sc on days 1 and 8 at the tail base with ALDH-A1, ALDH-A3, and CpG as either a soluble mixture or an (ALDH-A1/A3-CpG)-ND formulation (Figure 5A). Compared to the PBS control group, the soluble peptide mixture + CpG with or without anti-PD-L1 IgG therapy had no impact on 4T1 tumor growth or animal survival (Figure 5B–D). In stark contrast, NDs combined with anti-PD-L1 IgG exerted strong antitumor efficacy, leading to significantly slowed 4T1 tumor growth ($p < 0.0001$; Figure 5B,C) and prolonged animal survival ($p < 0.001$; Figure 5D) compared with soluble vaccine with or without anti-PD-L1 IgG. Using a subset of treatment groups, we quantified the frequency of residual ALDH^{high} CSCs in residual tumor tissues. ND vaccination combined with anti-PD-L1 IgG therapy significantly decreased the frequency of ALDH^{high} 4T1 CSCs compared with the PBS control group ($p < 0.05$) or the soluble vaccine plus anti-PD-L1 IgG group ($p < 0.01$; Figure 5E). Overall, these data indicated that (ALDH-A1/A3-CpG)-ND vaccination combined with anti-PD-L1 therapy had robust therapeutic effects against 4T1 breast cancer.

In summary, CSCs play crucial roles in cancer formation, metastasis, and recurrence and could potentially serve as a promising target for cancer treatment.[3–5] However, while chemotherapeutics and nucleic acid-based therapies have been assessed for killing CSCs,[35–37] it remains quite challenging to eliminate CSCs. In this study, we present a novel vaccination approach for eliminating CSCs. We identified ALDH-A1 and ALDH-A3 epitopes and developed nanodiscs (NDs) carrying these epitopes to induce ALDH-specific T cell responses. When combined with anti-PD-L1 IgG therapy, ND vaccination reduced the frequency of $ALDH^{high}$ CSCs in tumor tissues and exerted strong antitumor effects against multiple tumors known to harbor CSCs. While we and others have previously reported CSC lysate-based DC vaccines[12–14,38,39] or adoptive transfer of CSC-specific CD8+ T cells generated ex vivo,[40,41] this work represents the first demonstration of an off-the-shelf nanoparticle-based vaccine strategy against CSCs. We have previously reported that NDs can be used with patient-specific tumor neoantigens for personalized cancer immunotherapy.[28,29] Despite their promise, the identification and discovery of neoantigens from cancer patients as well as customized manufacturing of neoantigens present major technical and regulatory challenges to overcome.[42,43] On the other hand, since ALDH is a metabolic enzyme expressed in CSCs across a wide variety of cancer types,[6–11] our ND-based ALDH vaccination may offer a novel and universal pathway for immunological targeting and elimination of CSCs across many tumor types. While these proof-of-concept studies show the potential of ND vaccination, safety and off-target effects of ND vaccination against ALDH should be examined closely. In addition, more research is warranted to understand how reduction in the frequency of CSCs leads to tumor regression and how ND vaccination affects non-CSCs within tumor tissues. Overall, the therapeutic approach outlined here may open a new pathway for killing CSCs and should be evaluated further in the context of combination therapy to eliminate both CSCs and differentiated cancer cells.

EXPERIMENTAL SECTION

Reagents and Materials.

ALDH1-$A1_{88–96}$ (LLYKLADLI) and ALDH1-$A3_{99–107}$ (LLHQLADLV) epitope peptides modified with a cysteine at the N-terminus were synthesized by RS Synthesis (Louisville, KY). Female C57BL/6 mice aged 6–8 weeks were purchased from Jackson Laboratories (Bar Harbor, ME). Antibody against mouse PD-L1 was purchased from BioXCell (West Lebanon, NH). DMPC was purchased from NOF America (White Plains, NY). Peptide 22A mimetic was synthesized by GenScript (Piscataway, NJ). DOPE-PDP was purchased from Avanti Polar Lipids (Alabaster, AL). Both cholesterol-modified and unmodified CpG1826 were synthesized by Integrated DNA Technologies (Coralville, IA). IFN-γ ELISPOT kits were purchased from Fisher Scientific (Hampton, NH). Cell medium was purchased from Invitrogen (Carlsbad, CA). The following antibodies for flow cytometry were purchased from BioLegend: anti-mouse CD8a-APC, anti-mouse CD45R (B220)-PE/Cy7, rat anti-mouse CD4-Brilliant Violet 605, anti-mouse CD3-FITC, rat anti-mouse F4/80-APC–CY7, and anti-mouse CD11c-FITC. MHC tetramer kit was purchased from MBL International Corporation (Woburn, MA). TMR-NHS was purchased from Thermo Fisher Scientific (Waltham, MA).

Synthesis and Characterization of NDs Carrying ALDH Peptides.

Lipid–peptide conjugates were prepared as previously reported.[29,44,45] To incorporate ALDH peptides into NDs, peptides were modified with a cysteine at the N-terminus, and cysteine-terminated peptides were reacted with DOPE-PDP (antigen peptide:DOPE-PDP molar ratio = 2:1) for 4 h on an orbital shaker in dimethylformamide (DMF). The conjugation efficiency of the reaction was calculated on the basis of the reduction in absorbance signal associated with DOPE-PDP as measured by HPLC/MS. NDs were prepared as previously reported.[29,44] To incorporate ALDH peptides into NDs, lipid–peptide conjugate dissolved in dimethyl sulfoxide (DMSO) was added to the ND solution, followed by incubation at room temperature for 1 h. After incubation, unincorporated lipid–peptide conjugate was separated using ultracentrifuge filtration (MilliporeSigma Amicon Ultra Centrifugal Filter, 10 kDa). The efficiency of lipid–peptide conjugate incorporation into NDs was measured by quantifying the amount of lipid–peptide conjugate remaining before and after filtration of NDs using reversed-phase HPLC/MS, as previously reported.[29,44,46] In some studies, peptides tagged with TMR (excitation/emission at ~540/560 nm) were used to prepare NDs carrying TMR-tagged peptides. To load CpG into NDs, cho-CpG (Integrated DNA Technologies) was added dropwise to antigen-loaded NDs, followed by incubation at room temperature for 1 h. The amount of CpG loaded into NDs was quantified by GPC on a TSKgel G3000SWxl column (7.8 mm i.d. × 30 cm, Tosoh Bioscience LLC). The hydrodynamic size and zeta potential of NDs were measured using a Zetasizer Nano ZSP system (Malvern Panalytical, Malvern, U.K.). The morphology of NDs was investigated by TEM after 10× dilution, followed by osmium tetroxide negative staining. All of the TEM images were obtained using a JEOL JEM 1200EX electron microscope equipped with an AMT XR-60 digital camera (Advanced Microscopy Techniques).

Lymph Node Drainage and Antigen Uptake Mediated by NDs.

Animals were cared for following the federal, state, and local guidelines. The University of Michigan, Ann Arbor is an AAALAC international accredited institution, and all work conducted on animals was done in accordance with and approved by the Institutional Animal Care and Use Committee (IACUC). For lymph node drainage studies, female C57BL/6 mice of age 6–8 weeks were immunized with free ALDH-A1-TMR or (ALDH-A1-TMR)-ND containing antigen peptide (15.5 nmol/mouse) in a volume of 100 μL by subcutaneous injection at the tail base. At the 24 h time point after injection, animals were euthanized. Different organs were harvested, and the TMR signal was measured with an IVIS optical imaging system (Caliper Life Sciences). Afterward, inguinal lymph nodes were ground and passed through a 70 μm cell strainer, washed two times with FACS buffer (1% BSA in PBS), and stained with the indicated antibodies, followed by flow cytometry analysis.

In Vivo Immunization Study.

For the studies in D5-tumor-bearing animals, C57BL/6 female mice of age 6–8 weeks were inoculated sc in the right flank with 5×10^4 D5 cells on day 0. For the studies in 4T1-tumor-bearing animals, BALB/c mice of age 6–8 weeks (Jackson Laboratories) were inoculated sc with 10^4 4T1 cells in the mammary fat pad on day 0. Tumor-bearing animals were then

immunized sc at the tail base on days 1 and 8 with ALDH peptides (A1 and A3, each 15.5 nmol/dose) and CpG (15 μg/dose) in either soluble or ND form. In some studies, anti-mouse αPD-L1 antibody (100 μg/mouse) was administered intraperitoneally on days 3, 5, 7, 10, 12, and 14. Tumor growth was observed every other day, and the tumor volume was calculated using the following equation: tumor volume = length × $(\text{width})^2 \times 0.5$. Animals were euthanized when the tumor size reached 1.5 cm in any dimension or when animals became moribund with >20% weight loss or ulceration.

Immunological Analyses.

Blood samples were collected from the submandibular vein of mice, and red blood cells were lysed with ammonium–chloride–potassium (ACK) lysis buffer. A tetramer staining assay was used to quantify the percentage of CSC antigen-specific $CD8a^+$ T cells among PBMCs as described previously.[47] Briefly, the peptide–MHC tetramer was made according to the manufacturer's instructions. PBMCs were isolated, washed with FACS buffer, and incubated with anti-CD16/32 blocking antibody. Cells were then incubated with tetramer for 1 h on ice followed by incubation with anti-mouse CD8a-APC for 20 min on ice. Cells were then washed twice with FACS buffer, resuspended in DAPI solution (2 μg/mL), and analyzed by flow cytometry. For IFN-γ ELISPOT analysis, 2×10^5 PBMCs were added to an anti-IFN-γ-coated 96-well immunospot plate. PBMCs were restimulated with ALDH peptides (A1 and A3) for 18 h at 37 °C, followed by washing and development of plates according to the manufacturer's instructions. For the intracellular cytokine staining assay, PBMCs were seeded at 2×10^6 cells/mL on a 96-well U-bottom plate and restimulated with 10 μg/mL antigen peptides for 18 h in the presence of a protein transport inhibitor, brefeldin A (BD Biosciences). Subsequently, cells were washed with ice-cold FACS buffer and then incubated with anti-CD16/32 for 10 min, followed by anti-CD8a, anti-CD4, and a fixable viability dye (efluor450) for 20 min on ice. The cells were then fixed/permeabilized and stained with anti-IFN-γ for 30 min on ice. After two washes with FACS buffer, the cells were resuspended in FACS buffer and analyzed by flow cytometry. In some studies, tumors were excised, cut into small pieces, and digested using collagenase/hyaluronidase for 30–40 min. A single-cell suspension was produced and used to detect the percentage of residual $ALDH^{high}$ D5 or 4T1 CSCs by ALDEFLUOR assay via flow cytometry as previously reported.[12–14]

Statistical Analysis.

Sample sizes were selected according to pilot experiments and previously published results in the literature. All of the animal studies were performed after randomization. Data were analyzed by one-way or two-way ANOVA followed by Tukey's multiple comparisons post-test or the log-rank Mantel–Cox test with Prism 8.0 (GraphPad Software). Statistical significance is indicated as follows: *, $p < 0.05$; **, $p < 0.01$; ***, $p < 0.001$; ****$p < 0.0001$. All values are reported as mean ± SEM.

Supplementary Material

Refer to Web version on PubMed Central for supplementary material.

ACKNOWLEDGMENTS

This work was supported in part by NIH (R01EB022563, R01CA210273, R01AI127070, and R01DK125087 to J.J.M. R21NS091555 and R01HL134569 to A.S. R35CA197585 to M.W.), the MTRAC for Life Sciences Hub, a UM Forbes Institute for Cancer Discovery Pilot Grant, the Emerald Foundation, the Gillson Longenbaugh Foundation (Q.L. and A.E.C.), and Breast Cancer Research Foundation (M.W.). J.J.M. was supported by an NSF CAREER Award (1553831). J.Z., F.L., and Y.Q. were supported in part by Hubei Cancer Hospital, the China Scholarship Council, and Wuhan Union Hospital, respectively. E.B.O. was supported by an NSERC Postdoctoral Fellowship and a CIHR Postdoctoral Fellowship. D.A. was supported by a Cancer Center Support Grant (P30 CA046592). Some figures were created by the authors using BioRender.com.

REFERENCES

(1). Reya T; Morrison SJ; Clarke MF; Weissman IL Stem cells, cancer, and cancer stem cells. Nature 2001, 414 (6859), 105–11. [PubMed: 11689955]

(2). Jordan CT; Guzman ML; Noble M Cancer stem cells. N. Engl. J. Med 2006, 355 (12), 1253–61. [PubMed: 16990388]

(3). Sales KM; Winslet MC; Seifalian AM Stem cells and cancer: an overview. Stem Cell Rev. 2007, 3 (4), 249–255. [PubMed: 17955391]

(4). Pattabiraman DR; Weinberg RA Tackling the cancer stem cells—what challenges do they pose? Nat. Rev. Drug Discovery 2014, 13 (7), 497–512. [PubMed: 24981363]

(5). Batlle E; Clevers H Cancer stem cells revisited. Nat. Med 2017, 23 (10), 1124–1134. [PubMed: 28985214]

(6). Pearce DJ; Taussig D; Simpson C; Allen K; Rohatiner AZ; Lister TA; Bonnet D Characterization of cells with a high aldehyde dehydrogenase activity from cord blood and acute myeloid leukemia samples. Stem Cells 2005, 23 (6), 752–760. [PubMed: 15917471]

(7). Ginestier C; Hur MH; Charafe-Jauffret E; Monville F; Dutcher J; Brown M; Jacquemier J; Viens P; Kleer CG; Liu S; et al. ALDH1 is a marker of normal and malignant human mammary stem cells and a predictor of poor clinical outcome. Cell Stem Cell 2007, 1 (5), 555–567. [PubMed: 18371393]

(8). Silva IA; Bai S; McLean K; Yang K; Griffith K; Thomas D; Ginestier C; Johnston C; Kueck A; Reynolds RK; Wicha MS; Buckanovich RJ Aldehyde dehydrogenase in combination with CD133 defines angiogenic ovarian cancer stem cells that portend poor patient survival. Cancer Res. 2011, 71 (11), 3991–4001. [PubMed: 21498635]

(9). Marcato P; Dean CA; Giacomantonio CA; Lee PW Aldehyde dehydrogenase: its role as a cancer stem cell marker comes down to the specific isoform. Cell Cycle 2011, 10 (9), 1378–84. [PubMed: 21552008]

(10). Luo Y; Dallaglio K; Chen Y; Robinson WA; Robinson SE; McCarter MD; Wang J; Gonzalez R; Thompson DC; Norris DA; et al. ALDH1A isozymes are markers of human melanoma stem cells and potential therapeutic targets. Stem Cells 2012, 30 (10), 2100–2113. [PubMed: 22887839]

(11). Liu S; Cong Y; Wang D; Sun Y; Deng L; Liu Y; Martin-Trevino R; Shang L; McDermott SP; Landis MD; Hong S; Adams A; D'Angelo R; Ginestier C; Charafe-Jauffret E; Clouthier SG; Birnbaum D; Wong ST; Zhan M; Chang JC; Wicha MS Breast cancer stem cells transition between epithelial and mesenchymal states reflective of their normal counterparts. Stem Cell Rep. 2014, 2 (1), 78–91.

(12). Ning N; Pan Q; Zheng F; Teitz-Tennenbaum S; Egenti M; Yet J; Li M; Ginestier C; Wicha MS; Moyer JS; Prince ME; Xu Y; Zhang XL; Huang S; Chang AE; Li Q Cancer stem cell vaccination confers significant antitumor immunity. Cancer Res. 2012, 72 (7), 1853–64. [PubMed: 22473314]

(13). Lu L; Tao H; Chang AE; Hu Y; Shu G; Chen Q; Egenti M; Owen J; Moyer JS; Prince ME; Huang S; Wicha MS; Xia JC; Li Q Cancer stem cell vaccine inhibits metastases of primary tumors and induces humoral immune responses against cancer stem cells. Oncoimmunology 2015, 4 (3), No. e990767. [PubMed: 25949905]

(14). Hu Y; Lu L; Xia Y; Chen X; Chang AE; Hollingsworth RE; Hurt E; Owen J; Moyer JS; Prince ME; Dai F; Bao Y; Wang Y; Whitfield J; Xia JC; Huang S; Wicha MS; Li Q Therapeutic Efficacy

of Cancer Stem Cell Vaccines in the Adjuvant Setting. Cancer Res. 2016, 76 (16), 4661–72. [PubMed: 27325649]

(15). Klein O; Schmidt C; Knights A; Davis ID; Chen W; Cebon J Melanoma vaccines: developments over the past 10 years. Expert Rev. Vaccines 2011, 10 (6), 853–73. [PubMed: 21692705]

(16). Topalian SL; Drake CG; Pardoll DM Immune checkpoint blockade: a common denominator approach to cancer therapy. Cancer Cell 2015, 27 (4), 450–61. [PubMed: 25858804]

(17). Sharma P; Allison JP Immune checkpoint targeting in cancer therapy: toward combination strategies with curative potential. Cell 2015, 161 (2), 205–14. [PubMed: 25860605]

(18). Topalian SL; Taube JM; Anders RA; Pardoll DM Mechanism-driven biomarkers to guide immune checkpoint blockade in cancer therapy. Nat. Rev. Cancer 2016, 16 (5), 275–87. [PubMed: 27079802]

(19). Robert C; Schachter J; Long GV; Arance A; Grob JJ; Mortier L; Daud A; Carlino MS; McNeil C; Lotem M; Larkin J; Lorigan P; Neyns B; Blank CU; Hamid O; Mateus C; Shapira-Frommer R; Kosh M; Zhou H; Ibrahim N; Ebbinghaus S; Ribas A Pembrolizumab versus ipilimumab in advanced melanoma. N. Engl. J. Med 2015, 372 (26), 2521–32. [PubMed: 25891173]

(20). Nam J; Son S; Park KS; Zou W; Shea LD; Moon JJ Cancer nanomedicine for combination cancer immunotherapy. Nat. Rev. Mater. 2019, 4, 398–414.

(21). Schatton T; Frank MH Antitumor immunity and cancer stem cells. Ann. N. Y. Acad. Sci 2009, 1176, 154–69. [PubMed: 19796244]

(22). Miao Y; Yang H; Levorse J; Yuan S; Polak L; Sribour M; Singh B; Rosenblum MD; Fuchs E Adaptive Immune Resistance Emerges from Tumor-Initiating Stem Cells. Cell 2019, 177 (5), 1172–1186. [PubMed: 31031009]

(23). Su W; Han HH; Wang Y; Zhang B; Zhou B; Cheng Y; Rumandla A; Gurrapu S; Chakraborty G; Su J; Yang G; Liang X; Wang G; Rosen N; Scher HI; Ouerfelli O; Giancotti FG The Polycomb Repressor Complex 1 Drives Double-Negative Prostate Cancer Metastasis by Coordinating Stemness and Immune Suppression. Cancer Cell 2019, 36 (2), 139–155. [PubMed: 31327655]

(24). Ginestier C; Hur MH; Charafe-Jauffret E; Monville F; Dutcher J; Brown M; Jacquemier J; Viens P; Kleer CG; Liu S; Schott A; Hayes D; Birnbaum D; Wicha MS; Dontu G ALDH1 Is a Marker of Normal and Malignant Human Mammary Stem Cells and a Predictor of Poor Clinical Outcome. Cell Stem Cell 2007, 1 (5), 555–567. [PubMed: 18371393]

(25). Charafe-Jauffret E; Ginestier C; Iovino F; Tarpin C; Diebel M; Esterni B; Houvenaeghel G; Extra JM; Bertucci F; Jacquemier J; Xerri L; Dontu G; Stassi G; Xiao Y; Barsky SH; Birnbaum D; Viens P; Wicha MS Aldehyde dehydrogenase 1-positive cancer stem cells mediate metastasis and poor clinical outcome in inflammatory breast cancer. Clin. Cancer Res. 2010, 16 (1), 45–55. [PubMed: 20028757]

(26). Marcato P; Dean CA; Pan D; Araslanova R; Gillis M; Joshi M; Helyer L; Pan L; Leidal A; Gujar S; Giacomantonio CA; Lee PW Aldehyde dehydrogenase activity of breast cancer stem cells is primarily due to isoform ALDH1A3 and its expression is predictive of metastasis. Stem Cells 2011, 29 (1), 32–45. [PubMed: 21280157]

(27). Luo Y; Dallaglio K; Chen Y; Robinson WA; Robinson SE; McCarter MD; Wang J; Gonzalez R; Thompson DC; Norris DA; Roop DR; Vasiliou V; Fujita M ALDH1A isozymes are markers of human melanoma stem cells and potential therapeutic targets. Stem Cells 2012, 30 (10), 2100–13. [PubMed: 22887839]

(28). Kuai R; Li D; Chen YE; Moon JJ; Schwendeman A High-density lipoproteins: nature's multifunctional nanoparticles. ACS Nano 2016, 10 (3), 3015–3041. [PubMed: 26889958]

(29). Kuai R; Ochyl LJ; Bahjat KS; Schwendeman A; Moon JJ Designer vaccine nanodiscs for personalized cancer immunotherapy. Nat. Mater 2017, 16 (4), 489–496. [PubMed: 28024156]

(30). Melief CJ; Van Der Burg SH Immunotheray of established (pre) malignant disease by synthetic long peptide vaccines. Nat. Rev. Cancer 2008, 8 (5), 351–360. [PubMed: 18418403]

(31). Mei Y; Han X; Liu Y; Yang J; Sumagin R; Ji P Diaphanous-related formin mDia2 regulates beta2 integrins to control hematopoietic stem and progenitor cell engraftment. Nat. Commun 2020, 11 (1), 3172. [PubMed: 32576838]

(32). De Henau O; Rausch M; Winkler D; Campesato LF; Liu C; Cymerman DH; Budhu S; Ghosh A; Pink M; Tchaicha J; Douglas M; Tibbitts T; Sharma S; Proctor J; Kosmider N; White K; Stern H;

Soglia J; Adams J; Palombella VJ; McGovern K; Kutok JL; Wolchok JD; Merghoub T Overcoming resistance to checkpoint blockade therapy by targeting PI3Kgamma in myeloid cells. Nature 2016, 539 (7629), 443–447. [PubMed: 27828943]

(33). Kim RJ; Park JR; Roh KJ; Choi AR; Kim SR; Kim PH; Yu JH; Lee JW; Ahn SH; Gong G; Hwang JW; Kang KS; Kong G; Sheen YY; Nam JS High aldehyde dehydrogenase activity enhances stem cell features in breast cancer cells by activating hypoxia-inducible factor-2alpha. Cancer Lett. 2013, 333 (1), 18–31. [PubMed: 23174107]

(34). Zhuang X; Zhang W; Chen Y; Han X; Li J; Zhang Y; Zhang Y; Zhang S; Liu B Doxorubicin-enriched, ALDH(br) mouse breast cancer stem cells are treatable to oncolytic herpes simplex virus type 1. BMC Cancer 2012, 12, 549. [PubMed: 23176143]

(35). Shi S; Han L; Gong T; Zhang Z; Sun X Systemic delivery of microRNA-34a for cancer stem cell therapy. Angew. Chem., Int. Ed 2013, 52 (14), 3901–5.

(36). Sun TM; Wang YC; Wang F; Du JZ; Mao CQ; Sun CY; Tang RZ; Liu Y; Zhu J; Zhu YH; Yang XZ; Wang J Cancer stem cell therapy using doxorubicin conjugated to gold nanoparticles via hydrazone bonds. Biomaterials 2014, 35 (2), 836–45. [PubMed: 24144908]

(37). Shen S; Xia JX; Wang J Nanomedicine-mediated cancer stem cell therapy. Biomaterials 2016, 74, 1–18. [PubMed: 26433488]

(38). Wu D; Wang J; Cai Y; Ren M; Zhang Y; Shi F; Zhao F; He X; Pan M; Yan C; Dou J Effect of targeted ovarian cancer immunotherapy using ovarian cancer stem cell vaccine. J. Ovarian Res. 2015, 8, 68. [PubMed: 26497895]

(39). Duarte S; Momier D; Baque P; Casanova V; Loubat A; Samson M; Guigonis JM; Staccini P; Saint-Paul MC; De Lima MP; Carle GF; Pierrefite-Carle V Preventive cancer stem cellbased vaccination reduces liver metastasis development in a rat colon carcinoma syngeneic model. Stem Cells 2013, 31 (3), 423–32. [PubMed: 23193035]

(40). Visus C; Wang Y; Lozano-Leon A; Ferris RL; Silver S; Szczepanski MJ; Brand RE; Ferrone CR; Whiteside TL; Ferrone S; DeLeo AB; Wang X Targeting ALDH(bright) human carcinoma-initiating cells with ALDH1A1-specific CD8(+) T cells. Clin. Cancer Res. 2011, 17 (19), 6174–84. [PubMed: 21856769]

(41). Deng Z; Wu Y; Ma W; Zhang S; Zhang YQ Adoptive Tcell therapy of prostate cancer targeting the cancer stem cell antigen EpCAM. BMC Immunol. 2015, 16, 1. [PubMed: 25636521]

(42). Schumacher TN; Scheper W; Kvistborg P Cancer Neoantigens. Annu. Rev. Immunol 2019, 37, 173–200. [PubMed: 30550719]

(43). Scheetz L; Park KS; Li Q; Lowenstein PR; Castro MG; Schwendeman A; Moon JJ Engineering patient-specific cancer immunotherapies. Nat. Biomed Eng. 2019, 3 (10), 768–782. [PubMed: 31406259]

(44). Kuai R; Sun X; Yuan W; Ochyl LJ; Xu Y; Hassani Najafabadi A; Scheetz L; Yu M-Z; Balwani I; Schwendeman A; Moon JJ Dual TLR agonist nanodiscs as a strong adjuvant system for vaccines and immunotherapy. J. Controlled Release 2018, 282, 131–139.

(45). Kuai R; Sun X; Yuan W; Xu Y; Schwendeman A; Moon JJ Subcutaneous Nanodisc Vaccination with Neoantigens for Combination Cancer Immunotherapy. Bioconjugate Chem. 2018, 29 (3), 771–775.

(46). Scheetz L; Kadiyala P; Sun X; Son S; Hassani Najafabadi A; Aikins M; Lowenstein PR; Schwendeman A; Castro MG; Moon JJ Synthetic High-density Lipoprotein Nanodiscs for Personalized Immunotherapy Against Gliomas. Clin. Cancer Res. 2020, 26, 4369–4380. [PubMed: 32439701]

(47). Ochyl LJ; Bazzill JD; Park C; Xu Y; Kuai R; Moon JJ PEGylated tumor cell membrane vesicles as a new vaccine platform for cancer immunotherapy. Biomaterials 2018, 182, 157–166. [PubMed: 30121425]

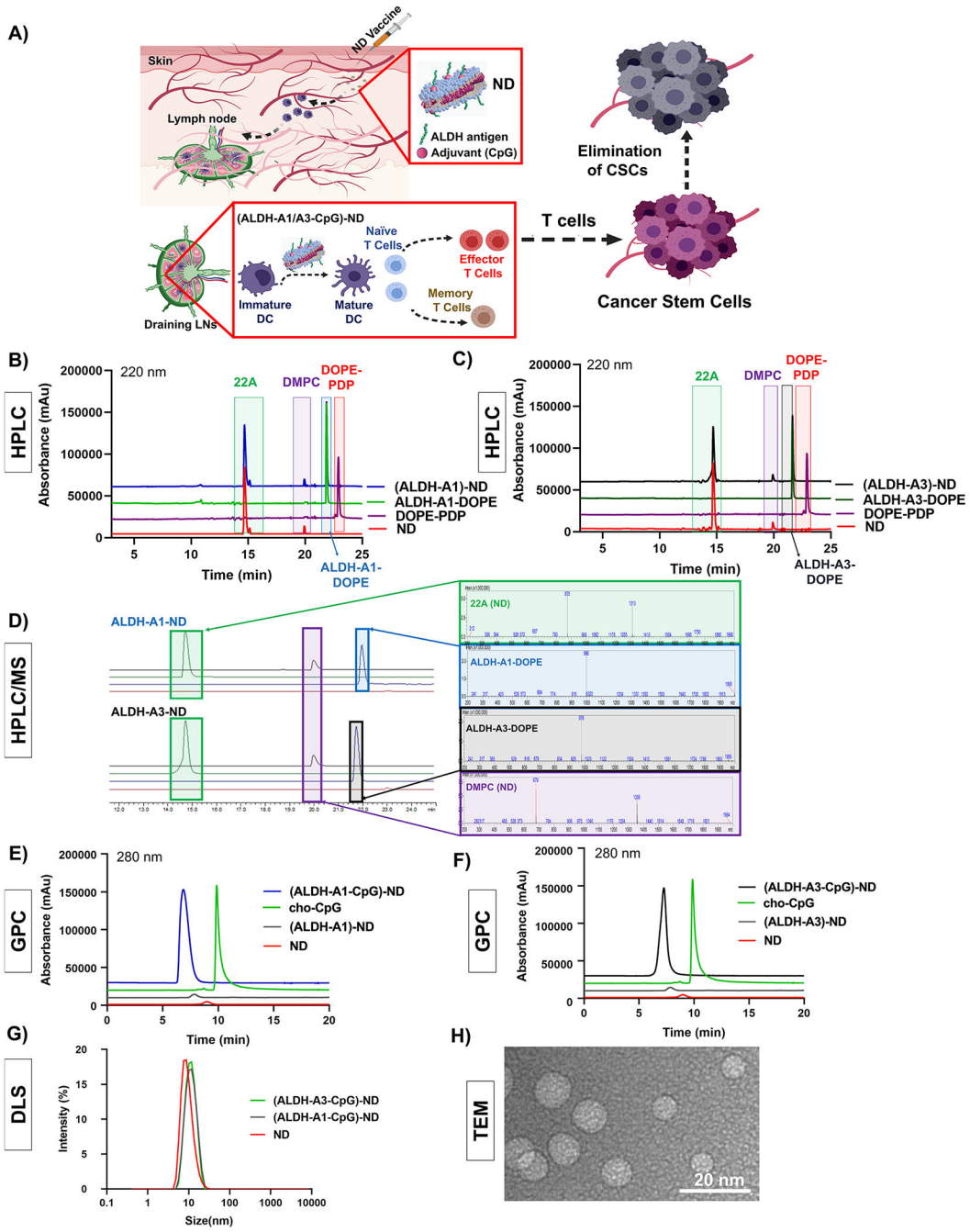

Figure 1.

Vaccination against cancer stem cells (CSCs) with nanodiscs (NDs) carrying ALDH epitopes. (A) Illustration of ND vaccination against ALDH^{high} CSCs. (B, C) HPLC chromatograms of (B) (ALDH-A1)-ND and (C) (ALDH-A3)-ND and their individual components. (D) HPLC/MS chromatograms indicating successful conjugation of ALDH-A1 and ALDH-A3 peptides to DOPE-PDP and subsequent incorporation of the lipid–peptide conjugates into NDs. (E, F) GPC chromatograms of (E) (ALDH-A1-CpG)-ND and (F) (ALDH-A3-CpG)-ND and their individual components. (G) DLS analyses of blank NDs,

(ALDH-A1-CpG)-ND, and (ALDH-A3-CpG)-ND. (H) TEM images of (ALDH-A1 or A3)-ND.

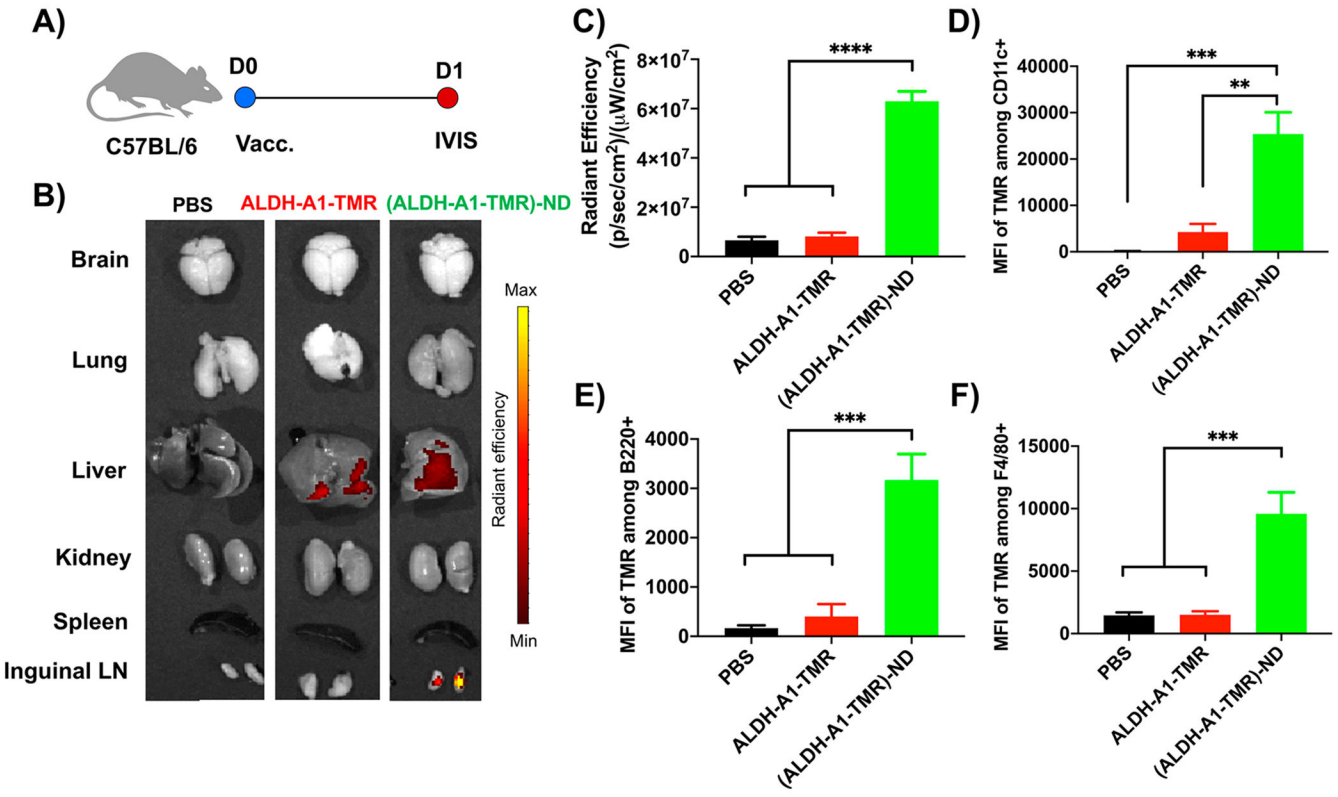

Figure 2.

NDs promote the delivery of ALDH peptides to APCs in draining lymph nodes. (A) TMR-tagged ALDH-A1 peptides (15.5 nmol) in soluble or ND form were administered sc to C57BL/6 mice. After 24 h, various organs were isolated, and the TMR signal was quantified. (B) Fluorescence images of major organs. (C) Quantification of the TMR signal in inguinal LNs. Data are presented as mean ± SEM ($n = 10$). (D–F) Antigen uptake by APCs in dLNs was quantified by flow cytometry analysis. Shown are MFI TMR signals among (D) $CD11c^+$ DCs, (E) $B220^+$ B cells, and (F) $F4/80^+$ macrophages in inguinal dLNs at 24 h after sc administration of (ALDH-A1-TMR)-ND or ALDH-A1-TMR. The data are shown as mean ± SEM. Statistical significance was calculated by one-way ANOVA followed by Tukey's multiple comparisons post-test: **, $p < 0.01$; ***, $p < 0.001$; ****, $p < 0.0001$.

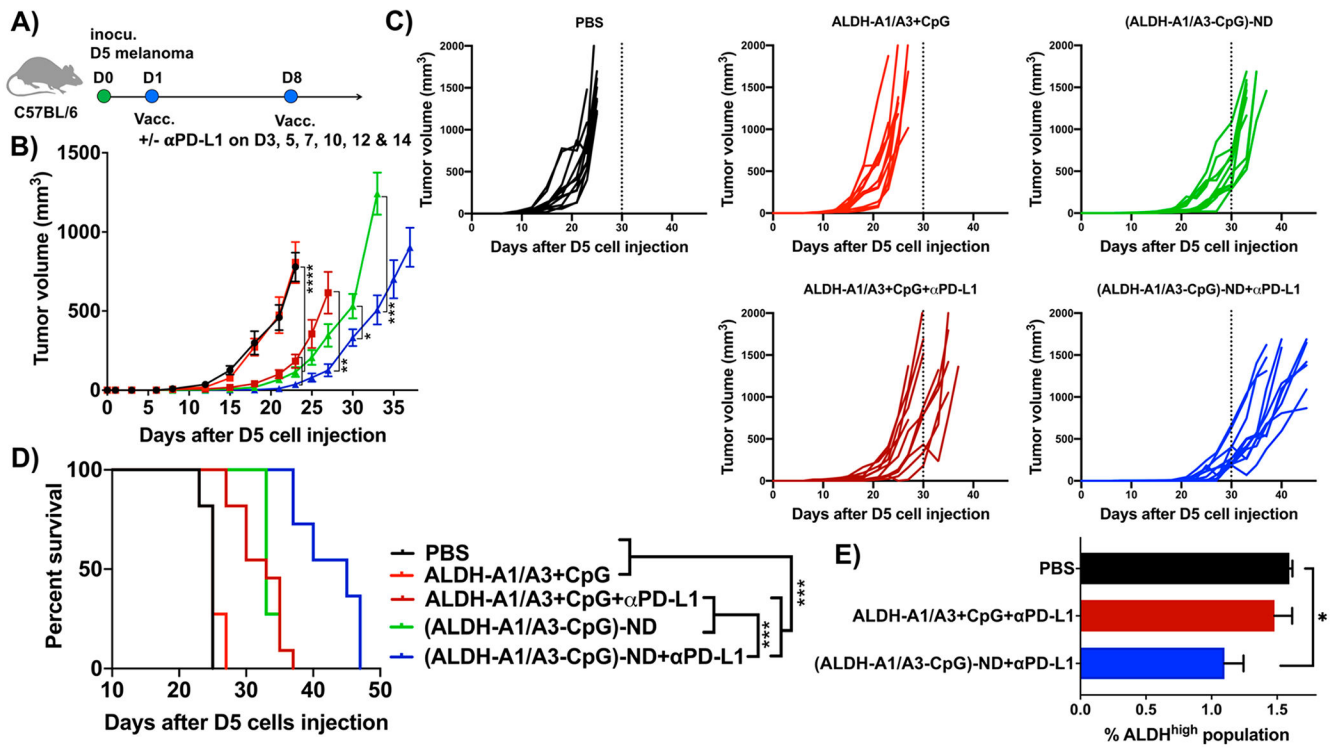

Figure 3.

Therapeutic efficacy of ALDH-ND vaccination in a D5 melanoma model. (A) C57BL/6 mice were inoculated sc in the flank with 5×10^4 D5 tumor cells and immunized with (ALDH-A1/A3-CpG)-ND or a soluble mixture of ALDH-A1/A3 and CpG (15.5 nmol/dose each antigen peptide and 15 μg/dose CpG) on days 1 and 8. A subset of mice also received ip administration of αPDL-1 (100 μg/dose) on the indicated days. Shown are (B) average tumor growth, (C) individual tumor growth, and (D) overall animal survival. (E) The frequency of $ALDH^{high}$ CSCs among live cells within the residual tumor masses was quantified on day 23. The data are shown as mean ± SEM. Statistical significance was calculated by (B) two-way ANOVA or (E) one-way ANOVA followed by Tukey's multiple comparisons post-test or (D) Kaplan–Meier survival analysis with the log-rank Mantel–Cox test: *, $p < 0.05$; **, $p < 0.01$; ***, $p < 0.001$; ****, $p < 0.0001$.

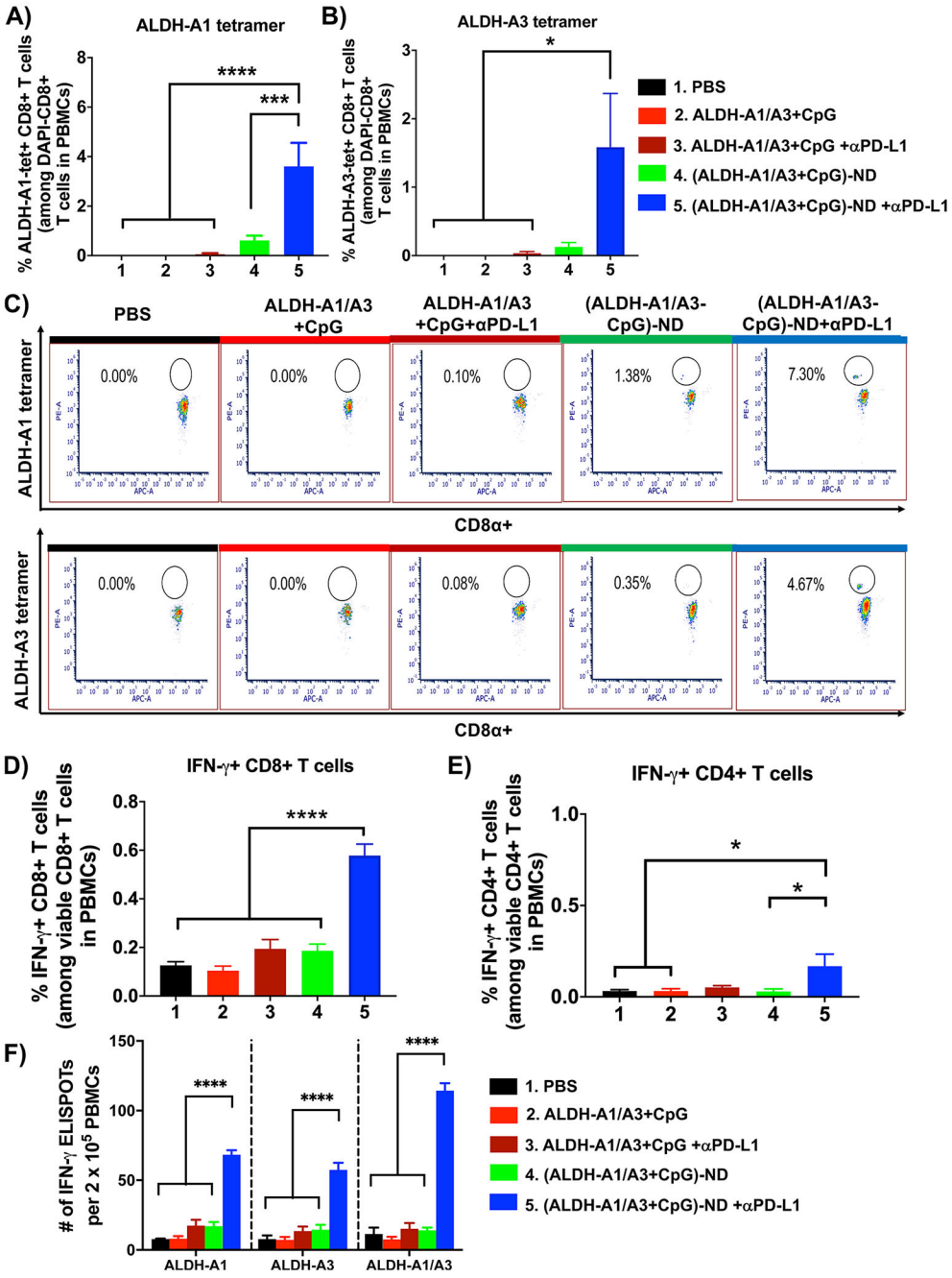

Figure 4.

ALDH-ND vaccination elicits potent T cell responses against ALDH^{high} CSCs. (A, B) Mice bearing D5 tumors were treated as in Figure 3A, and the frequencies of (A) ALDH-A1-specific and (B) ALDH-A3-specific CD8$^+$ T cells were quantified among PBMCs obtained on day 15. (C) Representative scatter plots of ALDH-A1 and ALDH-A3 tetramer+ CD8$^+$ T cells. (D, E) Frequencies of IFN-γ^+ (D) CD8$^+$ and (E) CD4$^+$ T cells as quantified by intracellular staining. (F) Results of an IFN-γ ELISPOT assay performed using PBMCs obtained on day 15 followed by ex vivo restimulation with the indicated peptides. The data

are shows as mean ± SEM. Statistical significance was calculated by (A, B, D, E) one-way ANOVA or (F) two-way ANOVA followed by Tukey's multiple comparisons post-test: *, $p < 0.05$; ***, $p < 0.001$; ****, $p < 0.0001$.

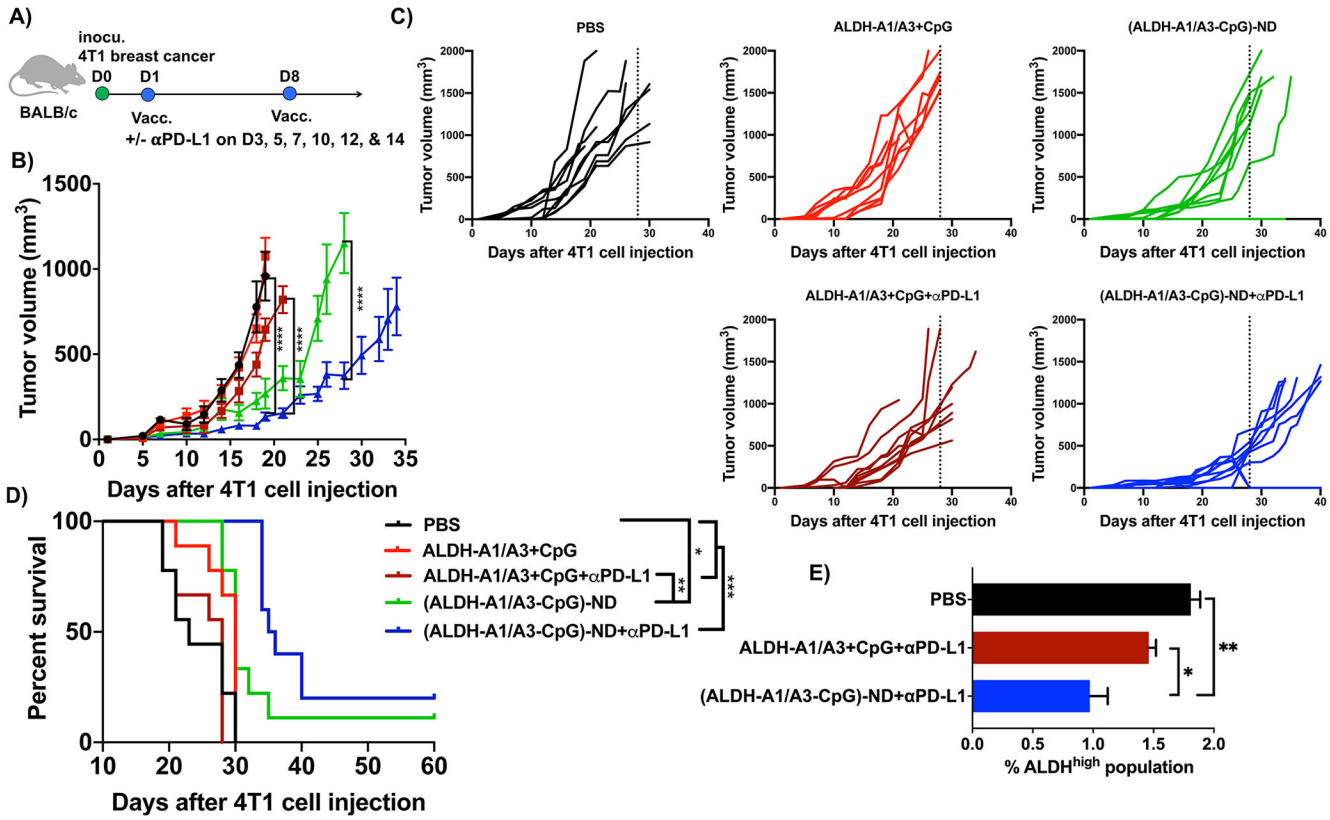

Figure 5.

Therapeutic efficacy of ALDH-ND vaccination in a 4T1 breast cancer model. (A) BALB/c mice were inoculated in the mammary fat pad with 10^4 4T1 tumor cells and immunized with (ALDH-A1/A3-CpG)-ND or a soluble mixture of ALDH-A1/A3 and CpG (15.5 nmol/dose each antigen peptide and 15 μg/dose CpG) on days 1 and 8. A subset of mice also received ip administration of αPDL-1 (100 μg/dose) on the indicated days. Shown are the (B) average tumor growth, (C) individual tumor growth, and (D) overall animal survival. (E) Frequencies of $ALDH^{high}$ CSCs among live cells within residual 4T1 tumor masses. The data are shown as mean ± SEM. Statistical significance was calculated by (B) two-way ANOVA or (E) one-way ANOVA followed by Tukey's multiple comparisons post-test or (D) Kaplan–Meier survival analysis with the log-rank Mantel–Cox test: *, $p < 0.05$; **, $p < 0.01$; ***, $p < 0.001$; ****, $p < 0.0001$.